

# Department of Mathematics and Statistics

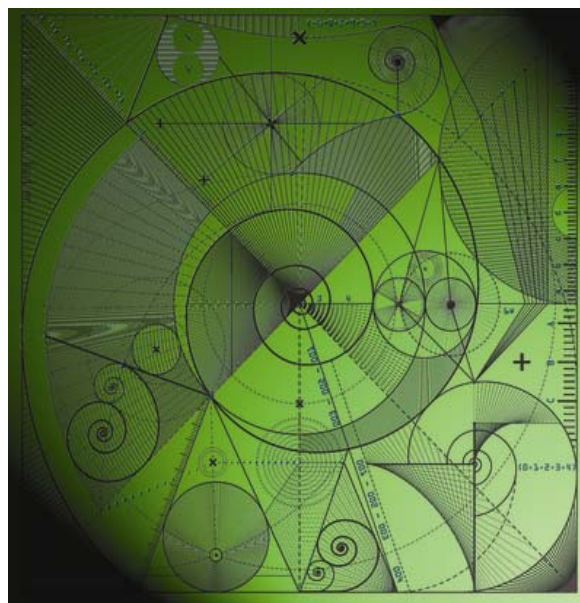
Preprint MPS-2012-12

11 June 2012

## Resolution of sharp fronts in the presence of model error in variational data assimilation

by

M.A. Freitag, N.K. Nichols and C.J. Budd





# Resolution of sharp fronts in the presence of model error in variational data assimilation

M. A. Freitag<sup>a\*</sup>, N. K. Nichols<sup>b</sup> and C. J. Budd<sup>a</sup>

<sup>a</sup>*Department of Mathematical Sciences, University of Bath, Claverton Down BA2 7AY, UK*

<sup>b</sup>*Department of Mathematics, The University of Reading, Box 220 Whiteknights, RG6 6AX, Reading, UK*

**Abstract:** We show that the four-dimensional variational data assimilation method (4DVar) can be interpreted as a form of Tikhonov regularisation, a very familiar method for solving ill-posed inverse problems. It is known from image restoration problems that  $L_1$ -norm penalty regularisation recovers sharp edges in the image more accurately than Tikhonov, or  $L_2$ -norm, penalty regularisation. We apply this idea from stationary inverse problems to 4DVar, a dynamical inverse problem, and give examples for an  $L_1$ -norm penalty approach and a mixed Total Variation (TV)  $L_1$ - $L_2$ -norm penalty approach. For problems with model error where sharp fronts are present and the background and observation error covariances are known, the mixed TV  $L_1$ - $L_2$ -norm penalty performs better than either the  $L_1$ -norm method or the strong-constraint 4DVar ( $L_2$ -norm) method. A strength of the mixed TV  $L_1$ - $L_2$ -norm regularisation is that in the case where a simplified form of the background error covariance matrix is used, it produces a much more accurate analysis than 4DVar. The method thus has the potential in numerical weather prediction to overcome operational problems with poorly tuned background error covariance matrices.

Copyright © 2010 Royal Meteorological Society

KEY WORDS Data assimilation; Tikhonov regularisation;  $L_1$  regularisation; TV regularisation, model error; linear advection equation

Received ; Accepted

## 1 Introduction

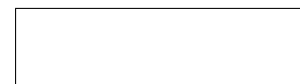
Data assimilation is a method for combining model forecast data with observational data in order to forecast more accurately the state of a system. One of the most popular data assimilation methods used in modern numerical weather prediction is four-dimensional variational data assimilation (4DVar) (Sasaki (1970); Talagrand (1981); Lewis *et al.* (2006)), which seeks initial conditions such that the forecast best fits both the observations and the background state (which is usually obtained from the previous forecast) within an interval called the assimilation window. Currently, in most operational weather centers, systems and states of dimension  $\mathcal{O}(10^7)$  or higher are considered, whereas there are considerably fewer observations, usually  $\mathcal{O}(10^6)$  (see Daley (1991); Nichols (2010) for reviews on data assimilation methods).

Linearised 4DVar can be shown to be equivalent to Tikhonov, or  $L_2$ -norm regularisation, a well-known method for solving ill-posed problems (Johnson *et al.* (2005)). Such problems appear in a wide range of applications (Engl *et al.* (1996)) such as geosciences and image restoration, the process of estimating an original image from a given blurred image. From the latter work it is known that by replacing the  $L_2$ -norm penalty term with an  $L_1$ -norm penalty function, image restoration becomes edge-preserving as the process does not penalise the edges of the image. The  $L_1$ -norm penalty regularisation

then recovers sharp edges in the image more precisely than the  $L_2$ -norm penalty regularisation (Hansen (1998); Hansen *et al.* (2006)). Edges in images lead to outliers in the regularisation term and hence,  $L_1$ -norms for the regularisation terms give a better result in image restoration. This is the motivation behind our approach for variational data assimilation.

The edge-preserving property of  $L_1$ -norm regularisation can be used for models that develop shocks, which is the case for moving weather fronts. In numerical weather prediction and ocean forecasting, it is recognized that the 4DVar assimilation method may not give a good analysis where there is a sharp gradient in the flow, such as a front (Bennett (2002); Lorenc (1981)). If the front is displaced in the background estimate, then the assimilation algorithm may smear the front and also underestimate the true amplitude of the shock (Johnson (2003)). In these cases the error covariances propagated implicitly by 4DVar are not representative of the correct error structures near the front. If model error is present, then there are systematic errors between the incorrect model trajectories and the observed data and therefore the strong constraint 4DVar, which assumes a perfect model, is not able to represent these errors correctly. Here we apply an  $L_1$ -norm penalty approach to several numerical examples containing sharp fronts for cases with model error. We show that the  $L_1$ -norm penalty approach applied to the gradient of the analysis vector (we call this mixed Total Variation (TV)  $L_1$ - $L_2$ -norm penalty regularisation) performs better than the standard  $L_2$ -norm regularisation in 4DVar. With the use of the gradient operator and the  $L_1$

\*Correspondence to: Department of Mathematical Sciences, University of Bath, Claverton Down BA2 7AY, UK. E-mail: m.freitag@maths.bath.ac.uk



norm, localisation of the gradient is enforced, which is important in tracking fronts. As an example we use the linear advection equation where sharp fronts and shocks are present. We use a numerical scheme that introduces some form of *model error* into the systems and find that, using an  $L_1$ -norm regularisation term, applied to the gradient of the solution, fronts are resolved more accurately than with the standard  $L_2$ -norm regularisation of 4DVar. Further investigation remains to be done in order to evaluate the technique in an operational setting.

Section 2 gives an introduction to 4DVar and shows its relation to Tikhonov regularisation. In Section 3 we introduce the new algorithms and in Section 4 we explain how we solve the  $L_1$ -norm regularisation problem and the mixed TV  $L_1$ - $L_2$ -norm regularisation problem. Sections 5 and 6 describe experiments using a linear advection model where the new regularisation approaches are compared with standard 4DVar for cases with model error. Under these conditions it is seen that mixed TV  $L_1$ - $L_2$ -norm regularisation outperforms 4DVar where sharp fronts are present. In the final section we present conclusions and discuss future work.

## 2 4DVar and its relation to Tikhonov regularisation

In nonlinear 4DVar we aim to minimise the objective function

$$\begin{aligned} \mathcal{J}(x_0) = & \frac{1}{2}(x_0 - x_0^b)^T B^{-1}(x_0 - x_0^b) \\ & + \frac{1}{2} \sum_{i=1}^N (y_i - \mathcal{H}_i(x_i))^T R_i^{-1}(y_i - \mathcal{H}_i(x_i)) \end{aligned} \quad (1)$$

subject to the system equations

$$x_{i+1} = \mathcal{M}_{i+1,i}(x_i), \quad i = 0, \dots, N-1. \quad (2)$$

This is a nonlinear constraint minimisation problem where the first term in (1) is called the background term,  $x_0^b$  is the background state at time  $t = 0$  and  $x_i \in \mathbb{R}^m$ ,  $i = 0, \dots, N$  are the state vectors at time  $t_i$ . The function  $\mathcal{M}_{i+1,i} : \mathbb{R}^m \rightarrow \mathbb{R}^m$  denotes the nonlinear model that evolves the state vector  $x_i$  at time  $t_i$  to the state vector  $x_{i+1}$  at time  $t_{i+1}$ . In weather forecasting the state vector  $x_0^b \in \mathbb{R}^m$  is the best estimate of the state of the system at the start of the window from the previous assimilation/forecast cycle. The vectors  $y_i \in \mathbb{R}^p$ ,  $i = 1, \dots, N$  contain the observations at times  $t_i$  and  $H_i : \mathbb{R}^m \rightarrow \mathbb{R}^p$  is the observation operator that maps the model state space to the observation space.

Minimising (1) is a weighted nonlinear least-squares problem. By minimising  $\mathcal{J}(x_0)$  we find an initial state  $x_0 \in \mathbb{R}^m$ , known as the *analysis*, such that the model trajectory is close to the background trajectory and to the observations in a suitable norm. The symmetric matrix  $B \in \mathbb{R}^{m,m}$  and the symmetric matrices  $R_i \in \mathbb{R}^{p,p}$ ,  $i = 1, \dots, N$  are assumed to represent the covariance matrices of the errors in the background and the observations respectively. The matrices  $R_i$  describe the combined

effects of measurement errors, representativity errors (arising from the need to interpolate state vectors to the times and locations of the observations) and errors in the observation operator. Provided the background and observation errors have Gaussian distributions with mean zero, then minimising  $\mathcal{J}(x_0)$  is equivalent to finding the *maximum a posteriori Bayesian estimate* of the true initial condition (Lorenz (1986)).

We apply a Gauß-Newton method (Dennis and Schnabel (1983)) in order to solve the minimisation problem (1). From a starting guess  $x_0^0$ , Newton's method for solving the gradient equation is

$$\nabla \nabla \mathcal{J}(x_0^k) \Delta x_0^k = -\nabla \mathcal{J}(x_0^k), \quad x_0^{k+1} = x_0^k + \Delta x_0^k, \quad (3)$$

for  $k \geq 0$ . In the Gauß-Newton method, the Hessian is replaced by an approximate Hessian  $\widetilde{\nabla \nabla \mathcal{J}(x_0^k)}$  that neglects all the terms involving second derivatives of  $\mathcal{M}_{i+1,i}$  and  $\mathcal{H}_i$ . We let  $M_{i+1,i}$  be the Jacobian of  $\mathcal{M}_{i+1,i}$ . Here we only consider problems where the observation operator is linear, that is  $\mathcal{H}_i(x_i) = H_i x_i$ . Furthermore, both  $R_i = R$  and  $H_i = H$ , are assumed to be unchanged over time.

The gradient of (1) is then given by

$$\begin{aligned} \nabla \mathcal{J}(x_0) = & B^{-1}(x_0 - x_0^b) \\ & - \sum_{i=1}^N M_{i,0}(x_0)^T H^T R^{-1}(y_i - H x_i), \end{aligned} \quad (4)$$

where  $M_{i,0}(x_0)$  is the Jacobian of  $\mathcal{M}_{i,0}(x_0)$ . The chain rule gives

$$M_{i,0}(x_0) = M_{i,i-1}(x_{i-1}) M_{i-1,i-2}(x_{i-2}) \cdots M_{1,0}(x_0). \quad (5)$$

Taking the gradient of (4) and neglecting terms involving the gradient of  $M_{i,0}(x_0)$  gives

$$\widetilde{\nabla \nabla \mathcal{J}(x_0)} = B^{-1} + \sum_{i=1}^N M_{i,0}(x_0)^T H^T R^{-1} H M_{i,0}(x_0). \quad (6)$$

Both the summation terms in (4) and (6) can be obtained recursively using the adjoint equations

$$\begin{aligned} \lambda_N &= 0, \\ \lambda_{i-1} &= M_{i,i-1}(x_{i-1})^T (\lambda_i + H^T R^{-1}(y_i - H x_i)), \end{aligned}$$

for  $i = N, \dots, 1$ , in order to find the gradient

$$\nabla \mathcal{J}(x_0) = B^{-1}(x_0 - x_0^b) - \lambda_0, \quad (7)$$

and similarly

$$\begin{aligned} \nabla \lambda_N &= 0 \\ \nabla \lambda_{i-1} &= M_{i,i-1}(x_{i-1})^T (\nabla \lambda_i - H^T R^{-1} H M_{i,0}(x_0)), \end{aligned}$$

for  $i = N, \dots, 1$ , leads to

$$\widetilde{\nabla \nabla \mathcal{J}(x_0)} = B^{-1} - \nabla \lambda_0. \quad (8)$$

Using these adjoint equations we avoid having to compute  $M_{i,i-1}(x_{i-1})$  several times. We note that  $\lambda_i, i = 0, \dots, N$  are vectors whereas  $\nabla\lambda_i, i = 0, \dots, N$  are square matrices of the dimension of the system state.

The approximate Hessian  $\nabla^2\mathcal{J}(x_0)$  and  $\nabla\mathcal{J}(x_0)$  are then used in (3), which is equivalent to a linearised least square problem. Here we solve this system directly. This approach is mathematically equivalent to the incremental 4DVar method as described in (Lawless *et al.* (2005a,b)); in the incremental method, however, the inner equations (3) are solved iteratively.

We may rewrite the objective function (1) in 4DVar as

$$\mathcal{J}(x_0) = \frac{1}{2}(x_0 - x_0^b)^T B^{-1}(x_0 - x_0^b) + \frac{1}{2}(\hat{y} - \hat{\mathcal{H}}(x_0))^T \hat{R}^{-1}(\hat{y} - \hat{\mathcal{H}}(x_0)), \quad (9)$$

where

$$\hat{\mathcal{H}}(x_0) = \begin{bmatrix} HM_{1,0}(x_0) \\ HM_{2,0}(x_0) \\ \vdots \\ HM_{N,0}(x_0) \end{bmatrix}, \quad \text{and} \quad \hat{y} = \begin{bmatrix} y_1 \\ y_2 \\ \vdots \\ y_N \end{bmatrix}.$$

In general  $\hat{\mathcal{H}}(x_0)$  is a nonlinear operator,  $\hat{y} \in \mathbb{R}^{pN}$  is a vector and  $\hat{R} \in \mathbb{R}^{pN,pN}$  is a block diagonal matrix with diagonal blocks equal to  $R$ . If we linearise  $M_{i,0}$  about  $x_0^b$ , then the Jacobian of the augmented matrix  $\hat{\mathcal{H}}$  is given by

$$\hat{H} := \hat{H}(x_0^b) = \begin{bmatrix} HM_{1,0}(x_0^b) \\ HM_{2,0}(x_0^b) \\ \vdots \\ HM_{N,0}(x_0^b) \end{bmatrix}, \quad (10)$$

which is essentially the observability matrix. Now writing  $B = \sigma_b^2 C_B$  and  $\hat{R} = \sigma_o^2 C_R$ , where  $C_B$  and  $C_R$  denote correlation matrices, and performing a variable transform  $z := C_B^{-1/2}(x_0 - x_0^b)$  we may write the linearised objective function that we aim to minimise as

$$\hat{J}(z) = \|C_R^{-1/2}(\hat{y} - \hat{\mathcal{H}}(x_0^b)) - C_R^{-1/2}\hat{H}C_B^{1/2}z\|_2^2 + \mu^2\|z\|_2^2, \quad \mu^2 = \frac{\sigma_o^2}{\sigma_b^2}. \quad (11)$$

This is equivalent to a linear least-squares problem with Tikhonov regularisation (Engl *et al.* (1996)), where  $\mu^2$  acts as the regularisation parameter. If we set

$$G := C_R^{-1/2}\hat{H}C_B^{1/2} \quad \text{and} \quad f := C_R^{-1/2}(\hat{y} - \hat{\mathcal{H}}(x_0^b)), \quad (12)$$

where  $G \in \mathbb{R}^{pN,m}$  and  $f \in \mathbb{R}^{pN}$ , then equation (11) may be written as

$$\min_z \hat{J}_2(z) = \min_z \{\|f - Gz\|_2^2 + \mu^2\|z\|_2^2\}, \quad \mu^2 = \frac{\sigma_o^2}{\sigma_b^2}. \quad (13)$$

If  $G$  is an ill-posed operator, or in the discrete setting an ill-conditioned matrix, then the minimisation problem

$$\min_z \{\|f - Gz\|_2^2\} \quad (14)$$

is hard to solve exactly, that is, the solution  $z$  does not continuously depend on the data. In data assimilation the matrix  $G$  is generally ill-conditioned, which means it has singular values that decay rapidly and many are very small or even zero. This problem occurs if there are not enough observations in the system, which is typical for numerical weather prediction. Furthermore, the given observations are subject to errors, leading to errors in the vector  $f$ . Hence, we can see that the minimisation problem (14) with an ill-conditioned system matrix  $G$  and an unreliable data vector  $f$  will lead to an unstable solution and some form of regularisation is required (for example preconditioning, Tikhonov regularisation, singular value filtering, etc.). We consider Tikhonov regularisation where a regularisation term  $\mu^2\|z\|_2^2$  is introduced, which leads to the objective function  $\hat{J}_2(z)$  in (13). The minimisation of the Tikhonov function (13) gives the regularised solution

$$z = (G^T G + \mu^2 I)^{-1} G^T f = \sum_{j=1}^{\min(pN,m)} \frac{\sigma_j^2}{\sigma_j^2 + \mu^2} \frac{u_j^T f}{\sigma_j} v_j, \quad (15)$$

where  $I \in \mathbb{R}^{m,m}$  is the identity matrix (see, for example, (Hansen *et al.*, 2006, Chapter 5) for details). The vectors  $u_j$  and  $v_j$  are the singular vectors of  $G$  belonging to the singular values  $\sigma_j$ , where  $G$  has the singular value decomposition  $G = U\Sigma V^T$ , with  $U \in \mathbb{R}^{pN,pN}$  and  $V \in \mathbb{R}^{m,m}$  being orthonormal matrices and  $\Sigma$  being a  $pN \times m$  matrix with entries  $\sigma_j \geq 0, j = 1, \dots, \min(pN, m)$ , on the leading diagonal and zeros elsewhere. Hence the factor  $\sigma_j^2/(\sigma_j^2 + \mu^2)$  acts as a filter factor for small singular values  $\sigma_j$ .

It is known from image processing (Hansen *et al.* (2006)) that instead of taking the  $L_2$ -norm for the regularisation term  $\mu^2\|z\|_2^2$  (that is the background term) the  $L_1$ -norm gives a better performance when sharp edges need to be recovered. The reason for the edge-preserving property of the  $L_1$ -norm is that the  $L_1$ -norm enforces a sparse solution (Donoho (2006a)). 4DVar performs poorly for the recovery of fronts. For shocks and fronts in the form of square waves or step functions, as in Figure 1 and all the following figures, the gradient of the solution is sparse and hence we introduce a mixed Total Variation  $L_1$ - $L_2$ -norm approach which aims to recover fronts and sparse solutions, see Wright *et al.* (2009). In general, the gradient would be small (but nonzero) away from the front, but  $L_1$  methods, which recover solutions with sparse gradients, should work well.

Hence we introduce and test two new approaches which are motivated by the  $L_1$ -norm regularisation and compare them to standard 4DVar: These are  $L_1$ -norm regularisation and a mixed Total Variation  $L_1$ - $L_2$ -norm regularisation. Both are described in the next section.

### 3 $L_1$ -norm and mixed $L_1$ - $L_2$ -norm regularisation

With the notation in (12), the minimisation problem in (11) can be written as (13) - known as standard Tikhonov regularisation - where the second term is a regularisation term and  $\mu^2$  is the regularisation parameter. In the literature, there has been a growing interest in using  $L_1$ -norm regularisation for image restoration, see, for example, [Fu et al. \(2006\)](#); [Agarwal et al. \(2007\)](#); [Schmidt et al. \(2007\)](#).

Firstly, in this paper we consider the effects of  $L_1$ -norm regularisation for variational data assimilation by replacing the squared  $L_2$ -norm in the regularisation term  $\mu^2 \|z\|_2^2$  of (13) by the  $L_1$ -norm to obtain

$$\min_z \hat{J}_1(z) = \min_z \{ \|f - Gz\|_2^2 + \mu^2 \|z\|_1 \}, \mu^2 = \frac{\sigma_o^2}{\sigma_b^2}. \quad (16)$$

Equation (13) can be written as

$$\min_z \hat{J}_2(z) = \min_z \left\{ \left\| \begin{bmatrix} f \\ 0 \end{bmatrix} - \begin{bmatrix} G \\ \mu I \end{bmatrix} z \right\|_2^2 \right\}, \mu^2 = \frac{\sigma_o^2}{\sigma_b^2}. \quad (17)$$

The minimisation problems (16) and (17) aim to produce a solution  $z$  and hence, with  $z := C_B^{-1/2}(x_0 - x_0^b)$ , an initial state  $x_0 = C_B^{1/2}z + x_0^b$  such that the solution trajectory is both close to the background (the previous forecast) and the observations in some weighted norm. The solution to problem (16) promotes sparsity in the solution, hence it promotes a sparse vector  $z$ . It has been shown that with very high probability the vector  $z$  if minimised in the  $L_1$  norm has very few entries (for further mathematical details of sparsity promoting minimisation we refer to [Donoho \(2006b\)](#)). We will see that this is generally not so useful for our computations.

Both the  $L_2$ -norm and the  $L_1$ -norm minimisation can be interpreted from a Bayesian point of view. For the  $L_2$ -norm approach - which is equivalent to standard 4DVar - a Gaussian distribution is assumed for the error in the prior, that is, for the background error. For the  $L_1$ -norm, the background error is assumed to have a Laplace (double-sided exponential) distribution. (For details, see the Appendix.)

The advantage of using the  $L_1$ -norm is that the solution is more robust to outliers. It has been observed that a small number of outliers have less influence on the solution ([Fu et al. \(2006\)](#)). Edges in images lead to outliers in the regularisation term and, hence,  $L_1$ -norms for the regularisation terms give a better result in image restoration. This is the motivation behind our approach for variational data assimilation.

However, if it is known that fronts are present in the solution then the gradient of the solution will be sparse - hence the gradient of the initial state  $x_0$  will be sparse. If

we approximate the gradient by a matrix  $D$  given by

$$D = \begin{bmatrix} 1 & 0 & \dots & & \\ -1 & 1 & 0 & \dots & \\ 0 & -1 & 1 & 0 & \dots \\ & \ddots & \ddots & \ddots & \\ \dots & 0 & -1 & 1 & \end{bmatrix}, \quad (18)$$

then the minimisation problem for a sparse initial state and hence a sharp front becomes

$$\min_z \hat{J}_{TV}(z) = \min_z \left\{ \left\| \begin{bmatrix} f \\ 0 \end{bmatrix} - \begin{bmatrix} G \\ \mu I \end{bmatrix} z \right\|_2^2 + \delta \|Dx_0\|_1 \right\}, \mu^2 = \frac{\sigma_o^2}{\sigma_b^2}, \quad (19)$$

where  $x_0 = C_B^{1/2}z + x_0^b$ ,  $D$  is given by (18) and  $\delta$  is another so-called regularisation parameter which needs to be chosen. The size of  $\delta$  determines how much sparsity is enforced on the gradient of the solution (see Table I for examples with different choices of  $\delta$ ). We will see in Section 5 that minimising  $\hat{J}_{TV}(z)$  in (19) gives a much better resolution of the fronts than minimising  $\hat{J}_2(z)$  or  $\hat{J}_1(z)$  in (17) or (16). (We remark that other choices for the derivative approximation  $D$  can be taken, but (18) is commonly used.)

We find that, for fronts and shocks, regularisation with an added  $L_1$ -norm on the derivative of the initial condition in 4DVar gives much better results than the standard  $L_2$ -norm approach in the presence of model error. When an  $L_1$ -norm penalty term with a gradient as in (19) is added one often speaks of total variation (TV) regularisation ([Strong and Chan \(2003\)](#)). We call the problem in (19) a mixed TV  $L_1$ - $L_2$ -norm regularisation problem.

In the following section we explain how we solve the  $L_1$ -norm minimisation problem in (16) and the mixed TV  $L_1$ - $L_2$ -norm minimisation problem in (19).

### 4 Least mixed norm solutions

We consider the minimisation problems (16) and (19). In order to solve these least mixed norm solutions we use an approach introduced by ([Fu et al. \(2006\)](#)). Both problems (16) and (19) are solved in a similar way. We explain the algorithm using the minimisation problem (19), the application of the algorithm to problem (16) is similar.

First, with  $x_0 = C_B^{1/2}z + x_0^b$ , problem (19) can be formulated as

$$\min_z \left\{ \left\| \begin{bmatrix} f \\ 0 \end{bmatrix} - \begin{bmatrix} G \\ \mu I \end{bmatrix} z \right\|_2^2 + \delta \|D(C_B^{1/2}z + x_0^b)\|_1 \right\}. \quad (20)$$

We let

$$v = \delta D(C_B^{1/2}z + x_0^b),$$

and split  $v$  into its non-negative and non-positive parts  $v^+$  and  $v^-$ , that is

$$v = v^+ - v^-$$

and

$$v^+ = \max(v, 0), \quad v^- = \max(-v, 0).$$

Problem (20) can then be written as

$$\min_{z, v^+, v^-} \left\{ \left\| \begin{bmatrix} f \\ 0 \end{bmatrix} - \begin{bmatrix} G \\ \mu I \end{bmatrix} z \right\|_2^2 + 1^T v^+ + 1^T v^- \right\}. \quad (21)$$

subject to the constraints

$$\delta D(C_B^{1/2} z + x_0^b) = v^+ - v^-, \quad (22)$$

$$v^+, v^- \geq 0. \quad (23)$$

Here  $\mathbf{1}$  denotes the vector of all ones of appropriate size. This problem can then be written as

$$\min_w \left\{ \frac{1}{2} w^T H w + c^T w \right\} \quad (24)$$

subject to

$$E w = g \quad \text{and} \quad F w \geq 0, \quad (25)$$

where

$$w = \begin{bmatrix} z \\ v^+ \\ v^- \end{bmatrix}, \quad H = \begin{bmatrix} 2(G^T G + \mu^2 I) & 0 & 0 \\ 0 & 0 & 0 \\ 0 & 0 & 0 \end{bmatrix},$$

$$c = \begin{bmatrix} -2G^T f \\ 1 \\ 1 \end{bmatrix}, \quad E = \begin{bmatrix} \delta D C_B^{1/2} & -I & I \end{bmatrix},$$

$$F = \begin{bmatrix} 0 & 0 & 0 \\ 0 & I & 0 \\ 0 & 0 & I \end{bmatrix}, \quad g = -\delta D x_0^b,$$

and the block matrices  $I$  and  $0$  as well as the vectors  $\mathbf{1}$  of all ones in the matrices  $H$ ,  $E$ ,  $F$  and  $c$  are of appropriate size. The objective function in (24) is convex as  $H$  is symmetric positive semi-definite. In order to solve the quadratic programming problem (24) with constraints (25) we use the MATLAB in-built function `quadprog.m`, which readily solves problems of the form (24),(25). For our problem we use an active-set quadratic programming strategy (also known as a projection method), which is described in Gill *et al.* (1981). For details on the implementation of the MATLAB quadratic programming tool we refer to the MATLAB Product Documentation Matlab (R2012a).

In the following sections we consider a square wave propagated by the linear advection equation as an example. We use a ‘true’ model (from which we take the observations) and another model, which is different from the truth and hence introduces a model error. For the different regularisation approaches we keep the regularisation parameter  $\mu$  fixed, as we are only investigating the influence of the norm in the regularisation term, but not the size of the regularisation parameter  $\mu$ . In all the examples we observe that the new edge-preserving mixed TV  $L_1$ - $L_2$ -norm regularisation indeed gives better results than the standard  $L_2$ -norm approach and the simple  $L_1$ -norm regularisation.

## 5 Numerical experiments

We consider the linear advection equation

$$u_t + u_x = 0, \quad (26)$$

on the interval  $x \in [0, 1]$ , with periodic boundary conditions. We discretise the equation using the upwind scheme

$$U_j^{n+1} = U_j^n - \frac{\Delta t}{\Delta x} (U_j^n - U_{j-1}^n), \quad (27)$$

where  $j = 1, \dots, N$ , and the CFL condition  $\Delta t < \Delta x$  needs to be satisfied for stability (see Morton and Mayers (2005); LeVeque (1992) for details). Note that the lower index in (27) is spatial and the upper index is temporal.

The initial solution is a square wave defined by

$$u(x, 0) = \begin{cases} 0.5, & 0.25 < x < 0.5 \\ -0.5, & x < 0.25 \quad \text{or} \quad x > 0.5. \end{cases} \quad (28)$$

This wave moves through the time interval; the true solution is obtained by the method of characteristics (by advecting the initial condition at speed 1, that is  $u(x, t) = u(x - t, 0)$ ). The model equations are defined by the upwind scheme (27) with boundary conditions  $U_0^n = U_N^n$ , where  $n = 1, \dots, 80$ ,  $N = 100$ ,  $\Delta x = \frac{1}{100}$  and  $n$  is the number of time steps. The same example is used in Griffith and Nichols (2000). For this example we take  $\Delta t = 0.005$ .

### 5.1 A standard experiment

We consider an assimilation window of length 40 time steps. After the assimilation period we compute the forecast for another 40 time steps, and hence, 80 time steps are considered in total. For the background and observation error covariance matrices we take  $B = 0.01I$  and  $R = 0.01I$ ; hence the background is given the same weight as a single observation in this case. Moreover, we choose the background to be equal to the truth given by (28) perturbed by Gaussian noise with mean zero and covariance  $B$ . The background thus contains errors with variance of order 0.01. We test several cases.

1. Perfect observations are taken everywhere in time and space.
2. Perfect observations are taken every 20 points in space and every 2 time steps.
3. Imperfect observations are taken every 20 points in space and every 2 time steps; for the observations we introduce Gaussian noise with mean zero and variance 0.01.

For all cases we test

- standard 4DVar (minimisation problem (17)),
- $L_1$ -norm regularisation (minimisation problem (16)), and
- mixed TV  $L_1$ - $L_2$ -norm regularisation (minimisation problem (19)).

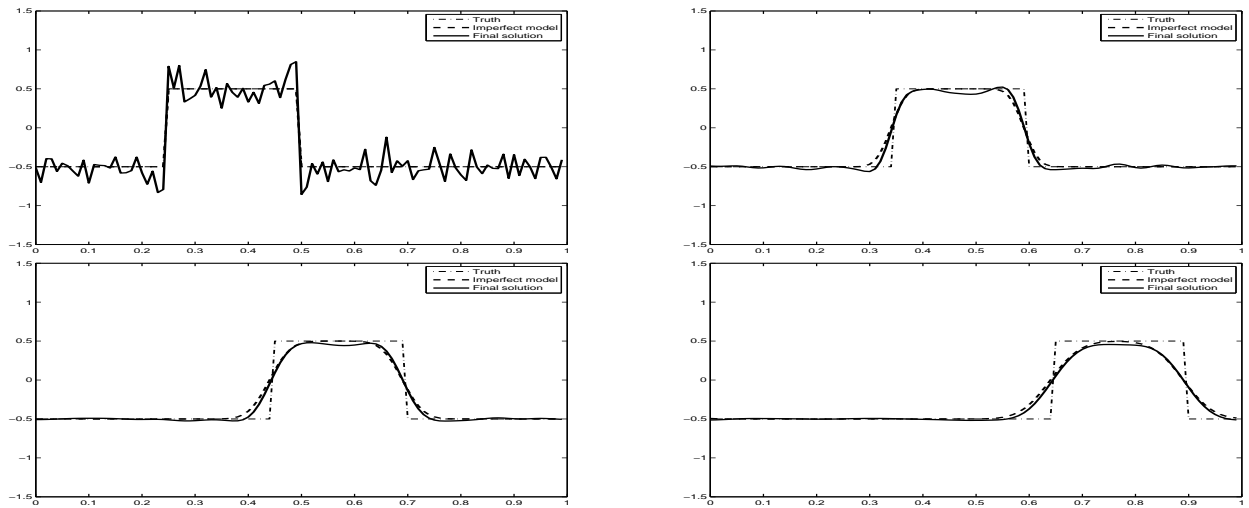


Figure 1. Results for **4DVar** applied to the linear advection equation where the initial condition is a square wave. We take **imperfect observations every 20 points in space and every 2 time steps**. 4DVar leads to bad oscillations in the initial condition and also to a phase error in the forecast.

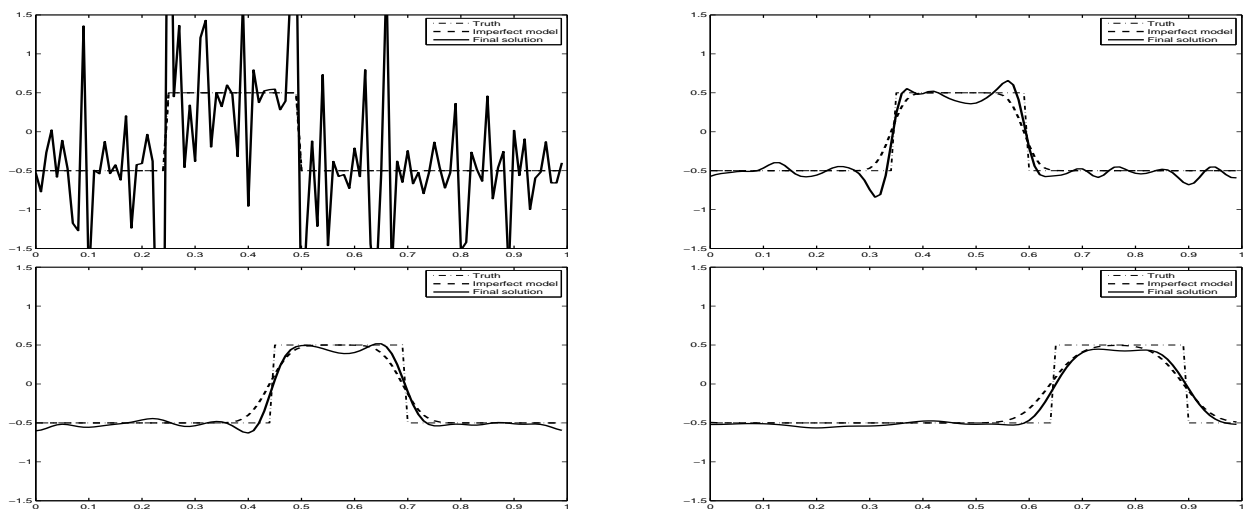


Figure 2. Results for  $L_1$  regularisation for the same data as in Figure 1.

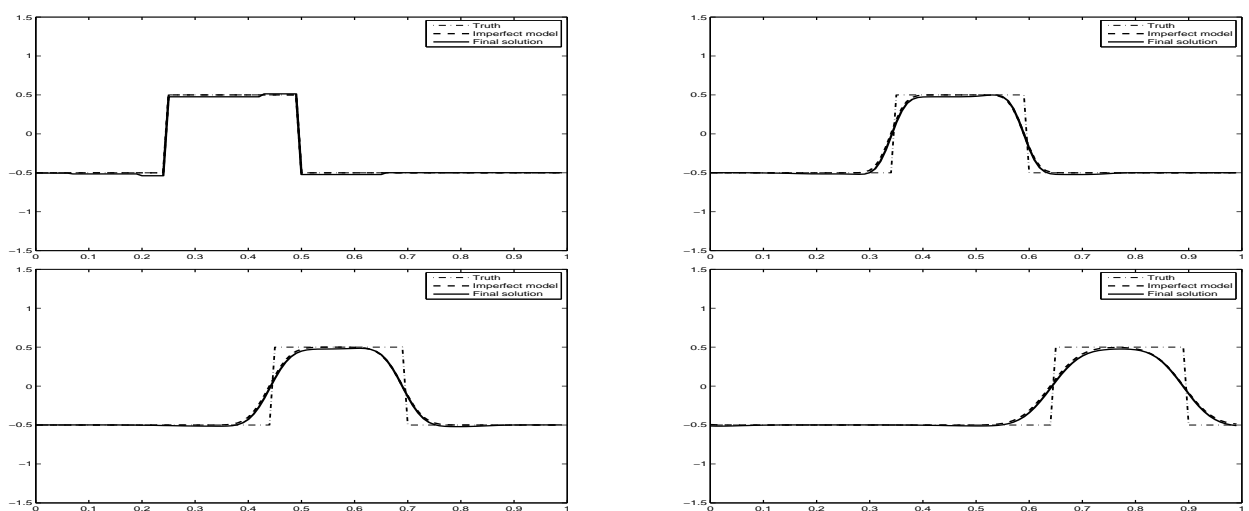


Figure 3. Results for **mixed TV  $L_1$ - $L_2$ -norm regularisation** for the same data as in Figure 1. Mixed TV  $L_1$ - $L_2$ -norm regularisation gives the best possible result for the initial condition.

Figures 1 - 3 show the results for this example. We only present the case for imperfect noisy observations, as it is the most realistic one. In the next subsection we consider a non-diagonal background error covariance matrix - for which we present the results for cases (1)-(3). We also note that a summary of results is presented in Table I.

In the plots the true solution is represented by a thick dot-dashed line (called 'Truth' in the legend). This true solution is unknown in practice. We take (noisy) observations by perturbing the true trajectory using zero-mean Gaussian noise. The model solution (which is derived from the upwind method) is shown as a dashed line (called 'Imperfect model' in the legend). This solution represents the model solution, that is the solution that is obtained if we use the correct initial conditions and the (imperfect) model. It represents the best solution that we are able to achieve (if data assimilation gives us the perfect initial condition), as the model error is always present. The solution obtained from the assimilation process by incorporating the (perfect/partial/noisy) observations is given by the solid line (called 'Final solution' in the legend).

The result for 4DVar is shown in Figure 1 (minimisation problem (17)), that for  $L_1$ -regularisation in Figure 2 (minimisation problem (16)) and that for mixed TV  $L_1$ - $L_2$ -norm regularisation in Figure 3 (minimisation problem (24)). The analysis obtained by 4DVar and  $L_1$ -regularisation is very inaccurate, with many oscillations and large over/undershoots near the discontinuities (first plots in Figures 1 and 2). When  $L_1$ -norm regularisation with the gradient (mixed TV  $L_1$ - $L_2$ -norm regularisation) is used, the initial condition is more accurate (first plot in Figure 3). The same results hold for full and partial perfect observations. The second row  $B = 0.01I$  of Table I quantifies the errors in the analysis for this situation for 4DVar,  $L_1$ -norm regularisation and the  $L_1$ -norm total variation approach. We see that for all types of observations we investigated (partial, full, perfect and noisy observations), mixed TV  $L_1$ - $L_2$ -norm regularisation gives the smallest initial condition error.

Traditional strong constraint 4DVar does not take model error into account. Hence 4DVar's attempts to compensate for the initial condition error are obstructed by the use of an imperfect forecast model and it therefore does not produce an accurate estimate of the truth at the initial time. The errors in the initial state estimated by 4DVar act to force the trajectory propagated by the incorrect model to match the observed data from the true model and hence act to compensate, on average, for the model error. From the final plot in Figure 1 for 4DVar we also see that the forecast is inaccurate, due to the incorrect estimate produced at the end of the assimilation window. We also observe that the forecast in 4DVar leads to a slight phase shift and the wrong amplitude in the forecast, as well as overshooting and undershooting. This behaviour is improved for mixed TV  $L_1$ - $L_2$ -norm regularisation (see Figure 3). We see from the first plot of Figure 3 that the initial condition obtained from mixed TV  $L_1$ - $L_2$ -norm regularisation is the most accurate and hence the best possible forecast (see final plot of Figure 3) is

obtained (subject to model error). This behaviour is due to the property of mixed TV  $L_1$ - $L_2$ -norm regularisation enforcing sparsity on the gradient of the solution.

The results shown in Figure 1 demonstrate a worst-case scenario for 4DVar, where there is no smoothing of the noisy analysis due to the use of the simple diagonal covariance matrix  $B$ . It is interesting to note, however, that, despite the lack of smoothing, the mixed TV  $L_1$ - $L_2$ -norm regularisation method (Figure 3) successfully eliminates oscillations in the analysis. From our experiments, it emerges that this is characteristic of this regularisation technique.

In the following subsections we change the experimental design in order to check the robustness of the regularisations. A more realistic matrix  $B$  is introduced in Subsection 5.2 and used in the following experiments. In Subsection 5.3 we investigate a change in the size of the assimilation window and in Subsection 5.4 we summarise the results from the different experimental designs. In Section 6 we assess the influence of 4DVar and mixed TV  $L_1$ - $L_2$ -norm regularisation on systems with different *a priori* background information.

## 5.2 Changing the background error covariance matrix

We take precisely the same experiments as in the previous Subsection 5.1; however, we change the background error covariance matrix from the identity matrix to an exponential covariance matrix  $B$  with entries

$$B_{ij} = \sigma_b^2 e^{-\frac{|i-j|}{2L^2}}, \quad \text{where } L = 5, \quad (29)$$

and  $\sigma_b^2 = 0.01$ . Hence  $B$  is a symmetric matrix with diagonal entries equal to 0.01 and off-diagonal entries that decay exponentially. This background error covariance matrix spreads the information from the observations more adequately and the error variance is still 0.01. Note that for this matrix the inverse is a tridiagonal matrix. For the background we choose Gaussian noise with covariance  $B$  and a mean value which is given by the truth. These errors are consistent with the choice of  $B$ .

We present the results for perfect, partial and imperfect partial observations (cases (1)-(3) in the description of the standard experiment in the previous subsection). Further cases are summarised in Table I in Subsection 5.4. We also do not present the results for  $L_1$  norm regularisation here as we have seen in Subsection 5.1 that this approach is not better than standard 4DVar. The more interesting case is the mixed TV  $L_1$ - $L_2$ -norm regularisation.

Figures 4 and 5 show the results for perfect observations where the background error covariance matrix  $B$  is given by (29). Mixed TV  $L_1$ - $L_2$ -norm regularisation (Figure 5) behaves consistently better than standard  $L_2$ -norm regularisation (Figure 4). In particular, the shape of the wave is distorted and there are small undershoots and overshoots in the 4DVar analysis (first plot in Figure 4), which lead to small errors and the wrong amplitude in the forecast (final plot in Figure 4). For the analysis using mixed TV  $L_1$ - $L_2$ -norm regularisation, the initial condition (first plot in Figure 5) shows a smaller error than the initial



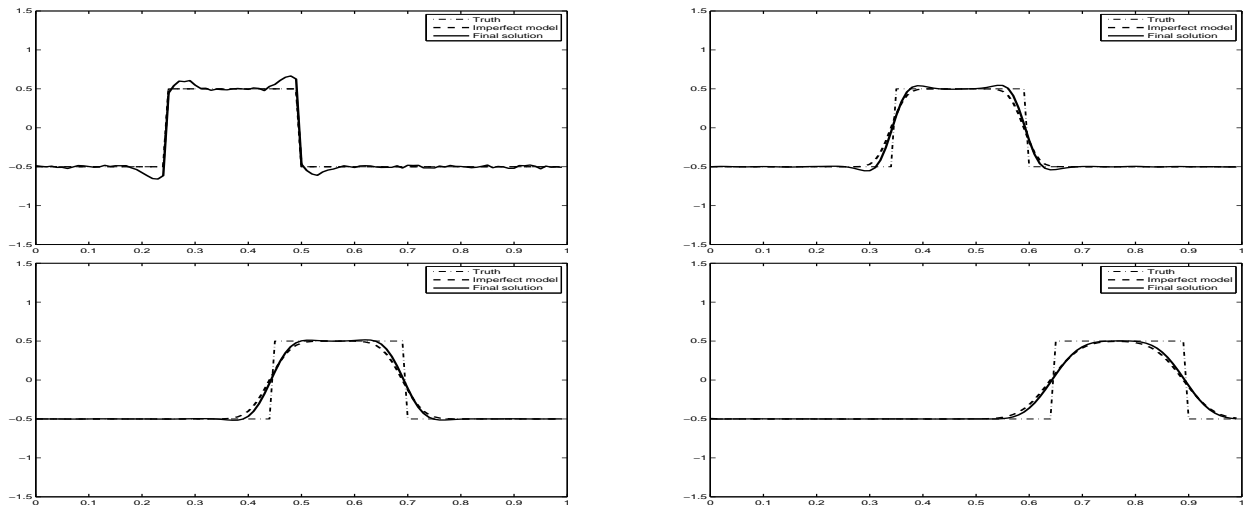


Figure 4. Results for **4DVar**. We take **perfect observations at each point in time and space** over the assimilation interval which is 40 time steps. The four plots show the initial conditions at  $t = 0$  and the result after 20, 40 and 80 time steps. We choose  $B$  with

$$B_{ij} = 0.01 e^{-\frac{|i-j|}{2L^2}}, \text{ where } L = 5.$$

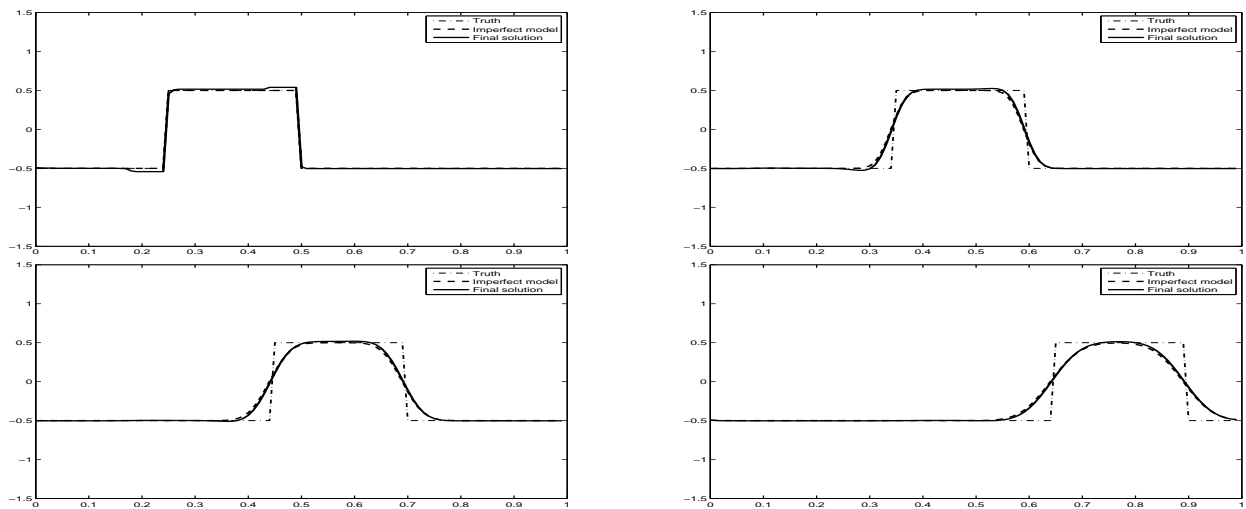


Figure 5. Results for **mixed TV  $L_1$ - $L_2$ -norm regularisation** for the same data as in Figure 4.

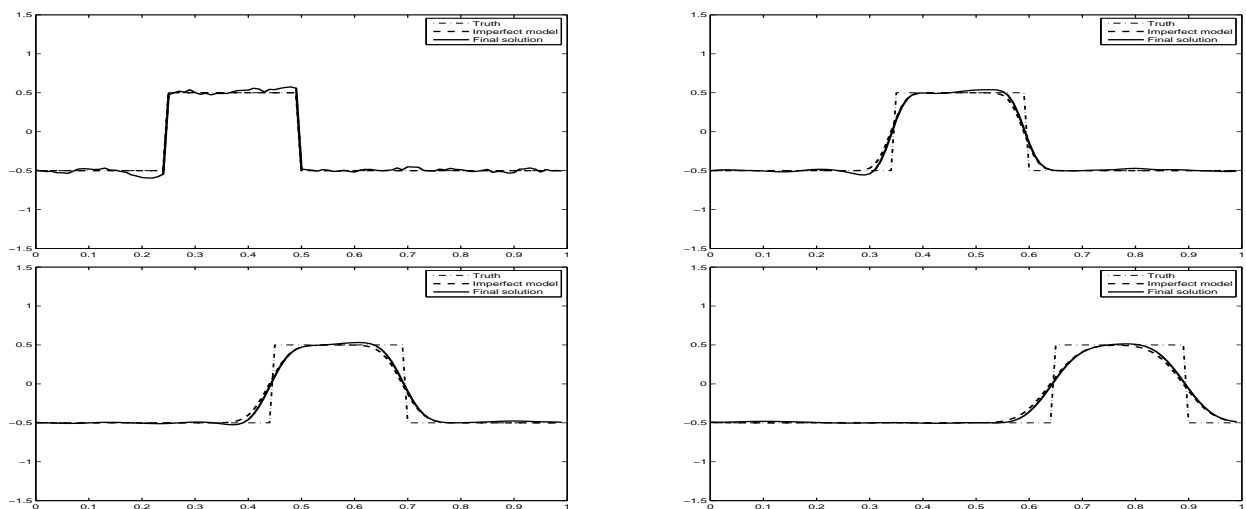


Figure 6. Results for **4DVar** for the same data as in Figure 4 but with **perfect observations every 20 points in space and every 2 time steps** for  $B$  with  $B_{ij} = 0.01 e^{-\frac{|i-j|}{2L^2}}$ , where  $L = 5$ .

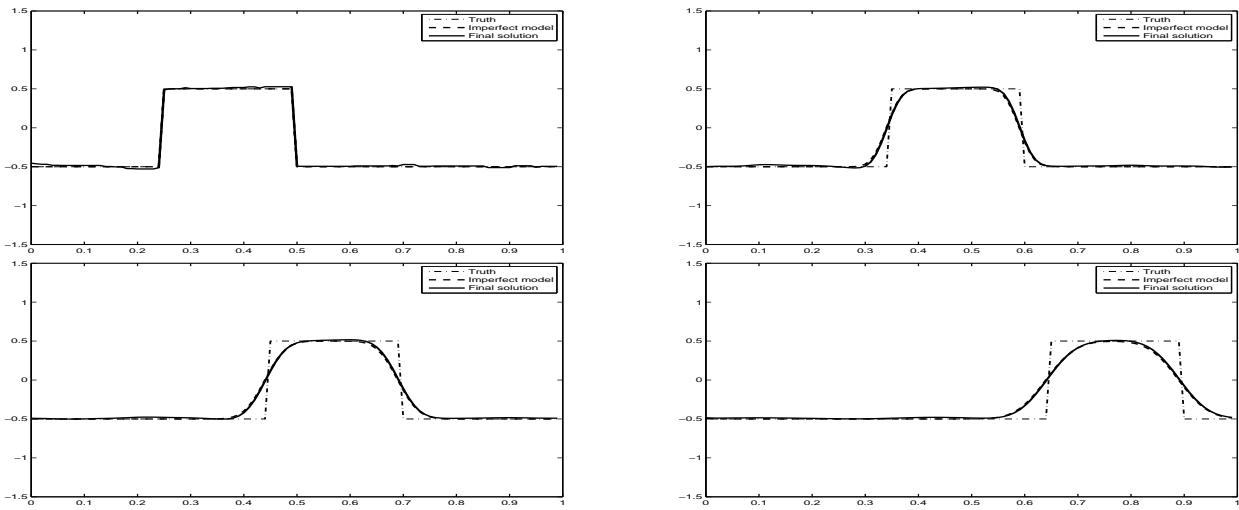


Figure 7. Results for mixed TV  $L_1$ - $L_2$ -norm regularisation for the same data as in Figure 6.

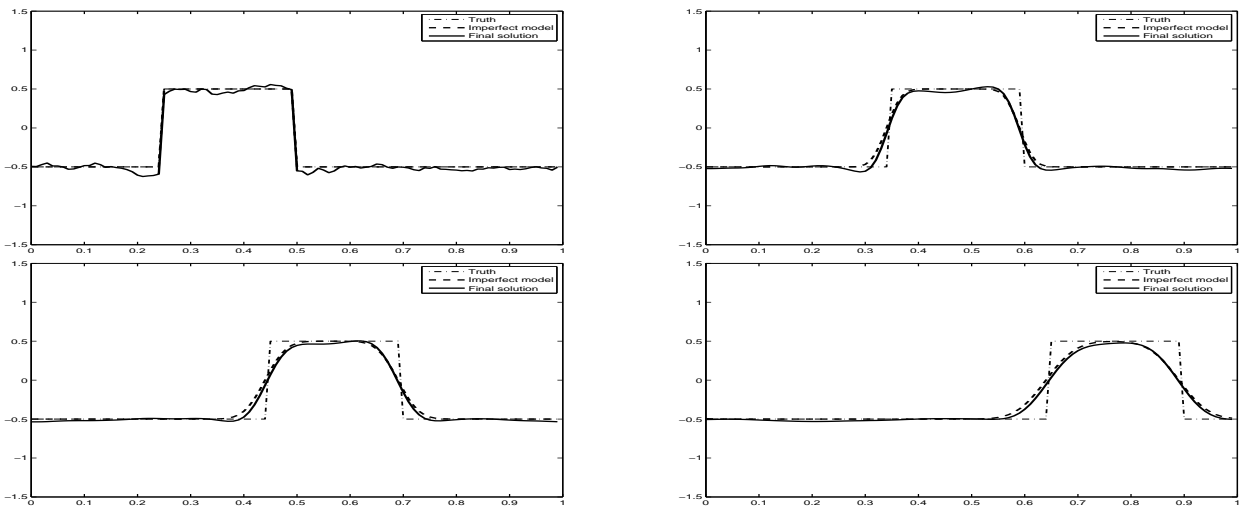


Figure 8. Results for 4DVar for the same data as in Figure 1, but for  $B$  with  $B_{ij} = 0.01 e^{-\frac{|i-j|}{2L^2}}$ , where  $L = 5$ .

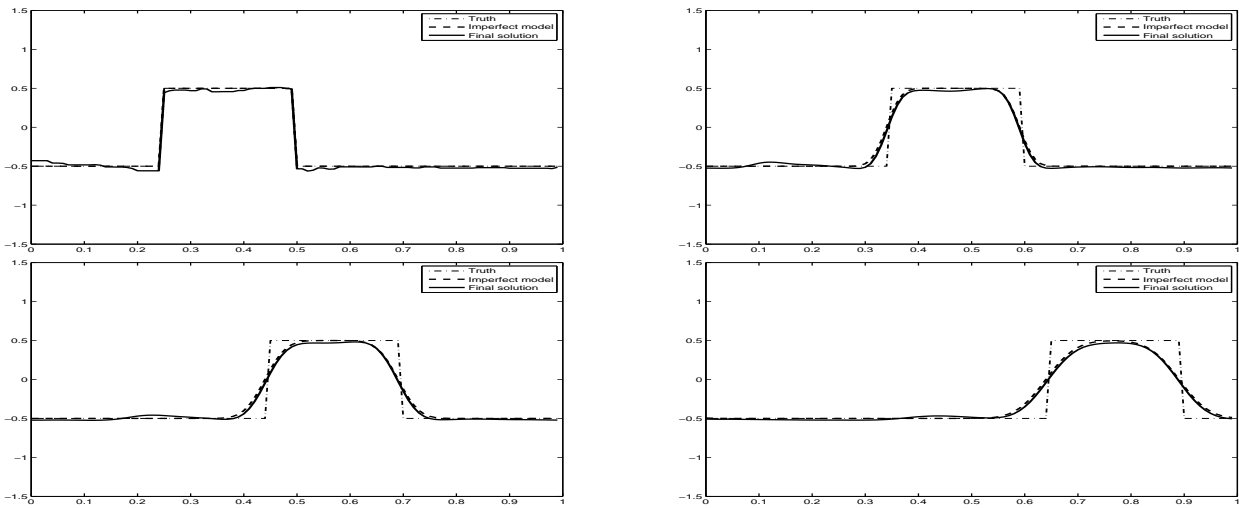


Figure 9. Results for mixed TV  $L_1$ - $L_2$ -norm regularisation for the same data as in Figure 8, but for  $B$  with  $B_{ij} = 0.01 e^{-\frac{|i-j|}{2L^2}}$ , where  $L = 5$

condition in standard 4DVar (first plot in Figure 4) and the forecast is slightly better than the forecast in 4DVar. For the case of partial perfect observations we obtain similar results. Mixed TV  $L_1$ - $L_2$ -norm regularisation (Figure 7) gives better initial conditions than standard 4DVar (Figure 6).

Finally, Figures 8 and 9 show the results for partial noisy observations. Note that with this choice of  $B$ , the results for 4DVar (Figure 8) are better than the results for the diagonal matrix  $B$  (Figure 1) because information is spread via the covariance matrix  $B$ , and we see that the oscillations in the analysis are significantly reduced. It is notable, however, that the mixed TV  $L_1$ - $L_2$ -norm regularisation (Figure 3) eliminates oscillations in the analysis even when the matrix  $B$  provides no smoothing. Moreover, where correlations are taken into account via the matrix  $B$ , then mixed  $L_1$ - $L_2$ -norm regularisation (Figure 9) gives still better results than 4DVar (Figure 8). The quantities of the errors in the initial conditions for this particular case are summarised in the fifth row of Table I where we see that the errors using mixed TV  $L_1$ - $L_2$ -norm regularisation are the smallest.

### 5.3 Changing the length of the assimilation window

Again, we take the same experimental data as in Subsection 5.1; this time, however, we reduce the size of the assimilation window from 40 time steps to 5 time steps and carry out the following test: we take imperfect observations every 5 points in space and every 2 time steps with Gaussian noise of mean zero and variance 0.01. For the background we again take the truth perturbed by Gaussian noise with covariance  $B$  taken from (29) with  $\sigma_b^2 = 0.01$ . Figures 10 and 11 show the results for a reduced size of the assimilation window. The first observation that we can make is that again the regularisation using the mixed TV  $L_1$ - $L_2$ -norm (Figure 11) is consistently better than that using the  $L_2$ -norm (Figure 10). Standard 4DVar produces oscillations, in particular in the initial conditions, whereas the mixed TV  $L_1$ - $L_2$ -norm regularisation does not show any oscillations. The oscillations in the initial conditions in standard 4DVar then lead to errors in the forecast (see plots for  $t = 5$ ,  $t = 20$  and  $t = 45$  in Figure 10). Again, for 4DVar, the forecast of the analysis does not keep the amplitude correctly (final plot in Figure 10), whereas the mixed TV  $L_1$ - $L_2$ -norm regularisation provides a more accurate amplitude in the forecast (final plot in Figure 11).

### 5.4 Summary of initial condition errors

In Table I we summarise the analysis errors (the errors between the analysis and the truth at  $t = 0$ , that is, the initial condition errors) measured in the  $L_2$  vector norm for the different regularisation techniques. The results are shown for all three test cases described in Section 5.1 where either perfect observations are taken at all spatial and time points, partial perfect observations are taken less frequently in time and space, or partial imperfect (noisy) observations are taken, also with less frequency.

We choose observation errors with covariance  $R = 0.01I$  and assimilation windows of length 40 and length 5. We consider the two background covariance matrices  $B = \sigma_b^2 I$ , and the double-sided exponential covariance matrix  $B$  given by (29), with three different variances:  $\sigma_b^2 = 1$ ,  $\sigma_b^2 = 0.01$  and  $\sigma_b^2 = 0.005$ .

For the mixed TV  $L_1$ - $L_2$ -norm regularisation method, we also give results for different values of  $\delta$  in (19). The emphasis on the sparsity of the gradient of the initial condition depends on this regularisation parameter. We have looked at three different values for  $\delta$  and the best of all three results (that is the smallest error in the initial condition) is underlined in the table. The regularisation depends on the regularisation parameter, but investigating the influence of this parameter and finding the optimal choice of  $\delta$  is beyond the scope of this paper. We remark that for the plots in the previous subsections we have used the value of  $\delta$  from the table that gives the smallest initial condition error.

We see from the entries in the table that the errors in the analysis at time  $t = 0$  are consistently smaller for mixed TV  $L_1$ - $L_2$ -norm regularisation than for standard 4DVar or  $L_1$ -norm regularisation. Mixed TV  $L_1$ - $L_2$ -norm regularisation gives an error of about one magnitude smaller than standard 4DVar. We also observe from the table that, for standard 4DVar,  $L_1$ -norm regularisation and mixed TV  $L_1$ - $L_2$ -norm regularisation, the errors in the initial condition (analysis) decrease as the variance in the background error is reduced, that is, as the ratio of the background to observation variance decreases. This is consistent with the results of Haben *et al.* (2010), which show that the standard 4DVar assimilation problem becomes more well-conditioned (well-posed) as this ratio decreases. These examples demonstrate that, even where the noise in the background and observations is Gaussian with known covariances, the standard 4DVar approach does not produce as accurate an analysis as mixed TV  $L_1$ - $L_2$ -norm regularisation in the presence of sharp fronts and model error.

## 6 Further experiments

We now investigate how the 4DVar and mixed TV  $L_1$ - $L_2$ -norm regularisation methods perform in cases where the position of the shock in the background is displaced from the truth and where the frontal gradient of an advected wave in the background is incorrect. As discussed in the introduction, it is recognized that if a shock in the background field is displaced, then the 4DVar method may not give a good analysis. Similarly, the assimilation method may be unable to capture a sharp shock if there is a weak gradient in the background front.

### 6.1 A shifted background

We consider the same problem as in Subsection 5.1 - with the same experimental data and error covariance matrices. However, here we shift the square wave in the background by 0.02 to the right, so that the shock is displaced. The

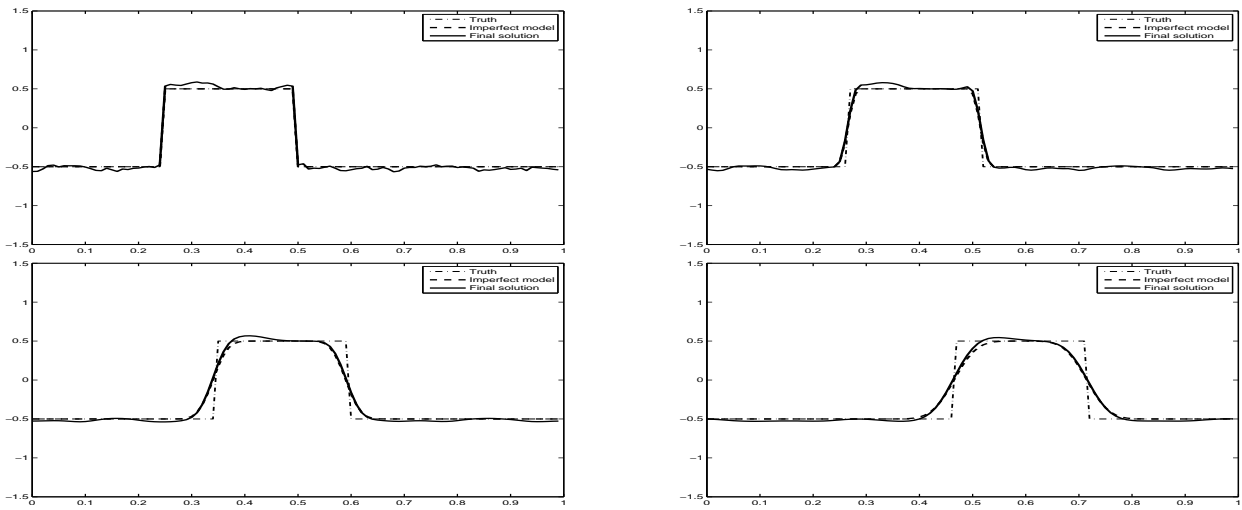


Figure 10. Results for **4DVar** applied to the linear advection equation where the initial condition is a square wave. We take **imperfect observations every 5 points in space and every 2 time steps** over the assimilation interval which is 5 time steps. The four plots show the initial conditions at  $t = 0$  and the result after 5, 20 and 45 time steps. 4DVar leads to oscillations in the initial condition and a misplaced discontinuity in the forecast.

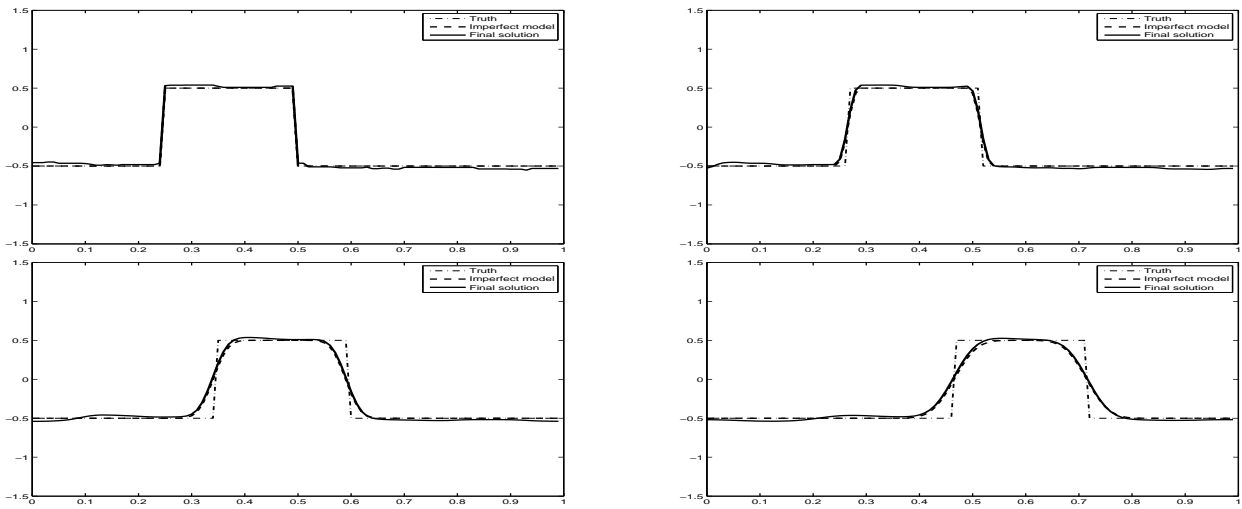


Figure 11. Results for **mixed TV  $L_1$ - $L_2$ -norm regularization** for the same data as in Figure 10. Mixed TV  $L_1$ - $L_2$ -norm regularization gives the best possible result for the initial condition.

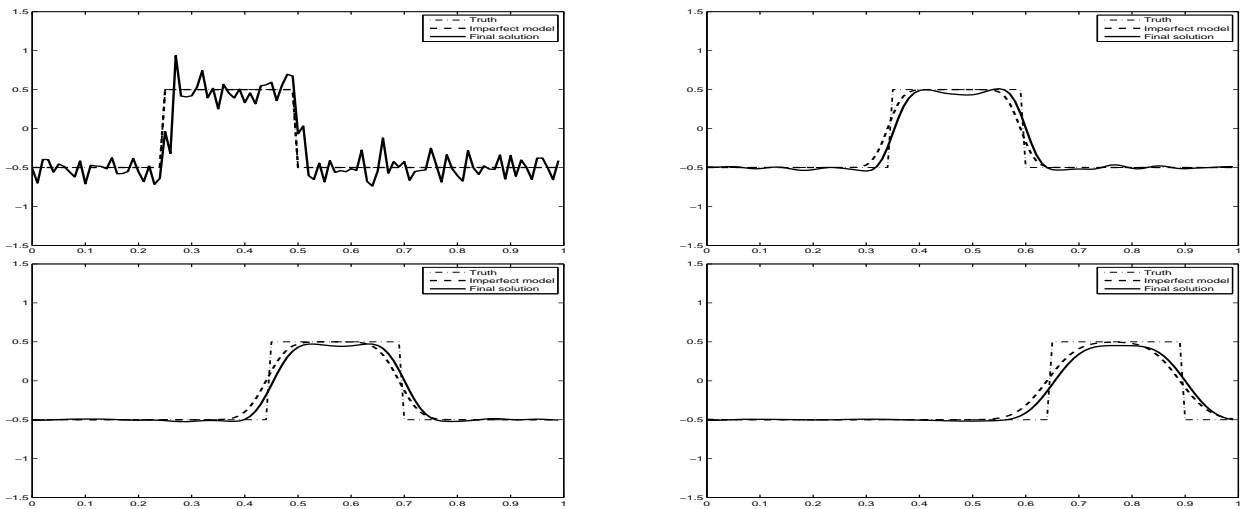


Figure 12. Results for **4DVar** for a shifted (and noisy) background and for background error covariance matrix  $B = 0.01I$

Table I. Comparison between errors in the analysis in standard 4DVar,  $L_1$ -norm regularisation and mixed TV  $L_1$ - $L_2$ -norm regularisation measured in the  $L_2$ -norm. Here the length-scale  $L = 5$ .

		Standard 4DVar	$L_1$ -norm regularisation	mixed TV $L_1$ - $L_2$ -norm regularisation		
				$\delta = 10$	$\delta = 100$	$\delta = 1000$
$B = I$	full perfect observations	2.3674	2.4392	1.1585	0.7674	0.2998
	partial perfect observations	12.8039	13.6598	9.3621	<u>0.4643</u>	2.7286
	partial imperfect observations	13.6182	14.4389	7.7128	<u>0.4790</u>	2.9110
$B = 0.01I$	full perfect observations	1.0609	1.4780	0.8963	0.6998	<u>0.2531</u>
	partial perfect observations	1.3791	10.0589	1.0935	<u>0.2866</u>	1.2440
	partial imperfect observations	1.4614	9.9083	1.0060	<u>0.1719</u>	1.3910
$B = 0.005I$	full perfect observations	0.9012	1.4567	0.7987	0.6417	<u>0.2272</u>
	partial perfect observations	0.8651	9.3547	0.6887	<u>0.2260</u>	0.8014
	partial imperfect observations	0.8979	8.5296	0.6566	<u>0.1500</u>	0.9141
$B$ with entries $B_{ij} = e^{-\frac{ i-j }{2L^2}}$	full perfect observations	1.1892	1.3703	0.9801	0.7391	<u>0.2807</u>
	partial perfect observations	2.7845	11.6647	2.2421	<u>0.3832</u>	2.7031
	partial imperfect observations	3.1041	11.1133	2.2780	<u>0.5552</u>	2.8524
$B$ with entries $B_{ij} = 0.01e^{-\frac{ i-j }{2L^2}}$	full perfect observations	0.4921	1.0184	0.4857	0.4346	<u>0.1696</u>
	partial perfect observations	0.3150	2.0667	0.2938	<u>0.1633</u>	0.9128
	partial imperfect observations	0.4161	1.5400	0.3997	<u>0.3057</u>	0.8456
$B$ with entries $B_{ij} = 0.005e^{-\frac{ i-j }{2L^2}}$	full perfect observations	0.4023	0.9396	0.3981	0.3636	<u>0.1567</u>
	partial perfect observations	0.2304	0.6327	0.2171	<u>0.1455</u>	0.6922
	partial imperfect observations	0.3225	0.5489	0.3139	<u>0.2680</u>	0.5686
$B = I$ and smaller length of assimilation window	full perfect observations	2.1595	2.1858	0.5812	<u>0.3406</u>	0.6591
	partial perfect observations	8.0773	8.2133	1.3201	<u>0.5327</u>	3.7108
	partial imperfect observations	11.2487	11.4258	1.6075	<u>0.6121</u>	3.6611
$B = 0.01I$ and smaller length of assimilation window	full perfect observations	0.6881	0.9963	0.4130	<u>0.1996</u>	0.4832
	partial perfect observations	0.9441	1.7047	0.6182	<u>0.2129</u>	1.6974
	partial imperfect observations	1.2017	2.5580	0.7971	<u>0.1795</u>	2.7750
$B = 0.005I$ and smaller length of assimilation window	full perfect observations	0.5463	0.8378	0.3677	<u>0.1553</u>	0.3939
	partial perfect observations	0.6809	1.4938	0.4903	<u>0.1795</u>	1.0246
	partial imperfect observations	0.8293	2.0489	0.6132	<u>0.1510</u>	1.1469
$B_{ij} = e^{-\frac{ i-j }{2L^2}}$ and smaller length of assimilation window	full perfect observations	0.8842	1.0369	0.5210	<u>0.2725</u>	0.6112
	partial perfect observations	1.2200	1.5908	0.7974	<u>0.3784</u>	3.6971
	partial imperfect observations	1.7078	2.6882	1.0445	<u>0.4655</u>	3.6392
$B_{ij} = 0.01e^{-\frac{ i-j }{2L^2}}$ and smaller length of assimilation window	full perfect observations	0.2256	0.2878	0.2166	<u>0.1558</u>	0.3266
	partial perfect observations	0.4688	0.5948	0.4533	<u>0.3000</u>	0.4088
	partial imperfect observations	0.3366	0.4790	0.3189	<u>0.2864</u>	1.1626
$B_{ij} = 0.005e^{-\frac{ i-j }{2L^2}}$ and smaller length of assimilation window	full perfect observations	0.1959	0.2204	0.1913	<u>0.1511</u>	0.2443
	partial perfect observations	0.3944	0.4887	0.3811	<u>0.2782</u>	0.9113
	partial imperfect observations	0.2770	0.3799	<u>0.2686</u>	0.2691	0.8676

reason for this shift is a practical one; fronts are often resolved correctly in numerical weather forecasting, but the front is often predicted to be in the wrong position. We simulate this situation in our simplified model by assuming a slightly shifted background. We add noise to this background, taken from a normal distribution with (1) a background error covariance matrix  $B = 0.01I$  and (2) a background error covariance matrix  $B$  taken from (29) with  $\sigma_b^2 = 0.01$  which is consistent with the error in the shifted background. We only consider the case with partial noisy observations, since this is the most interesting and realistic one.

The results for background error covariance matrix  $B = 0.01I$  are shown in Figures 12 (4DVar) and 13 (mixed TV  $L_1$ - $L_2$ -norm regularisation). We note that in the case of 4DVar the recovered analysis (first plot in

Figure 12) is very oscillatory and at the end of the window the solution contains undershoots (third plot in Figure 12), whereas in the analysis for the mixed TV  $L_1$ - $L_2$ -norm regularisation (first plot in Figure 13) the oscillations are removed and the front sharpened, although not recovered exactly. Furthermore, mixed TV  $L_1$ - $L_2$ -norm regularisation contains no undershoots at the end of the window and retains the amplitude of the front more accurately than 4DVar (see second and third plots in Figures 12 and 13). The errors in the analysis, measured in the  $L_2$ -norm, for the standard 4DVar method and for the mixed TV  $L_1$ - $L_2$ -norm regularisation (with  $\delta = 100$ ) are given respectively by 1.75 and 1.17, demonstrating the increased accuracy achieved by the new method.

The results for an exponential covariance matrix  $B$  with  $\sigma_b^2 = 0.01$  are shown in the plots in Figures 14

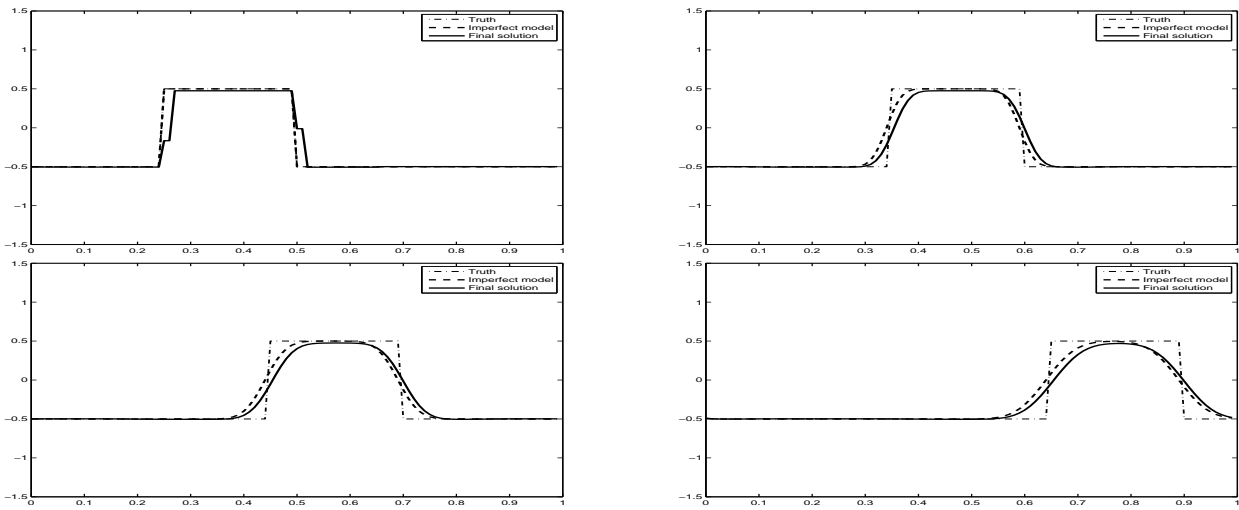


Figure 13. Results for mixed TV  $L_1$ - $L_2$ -norm regularisation for the same data as in Figure 12.

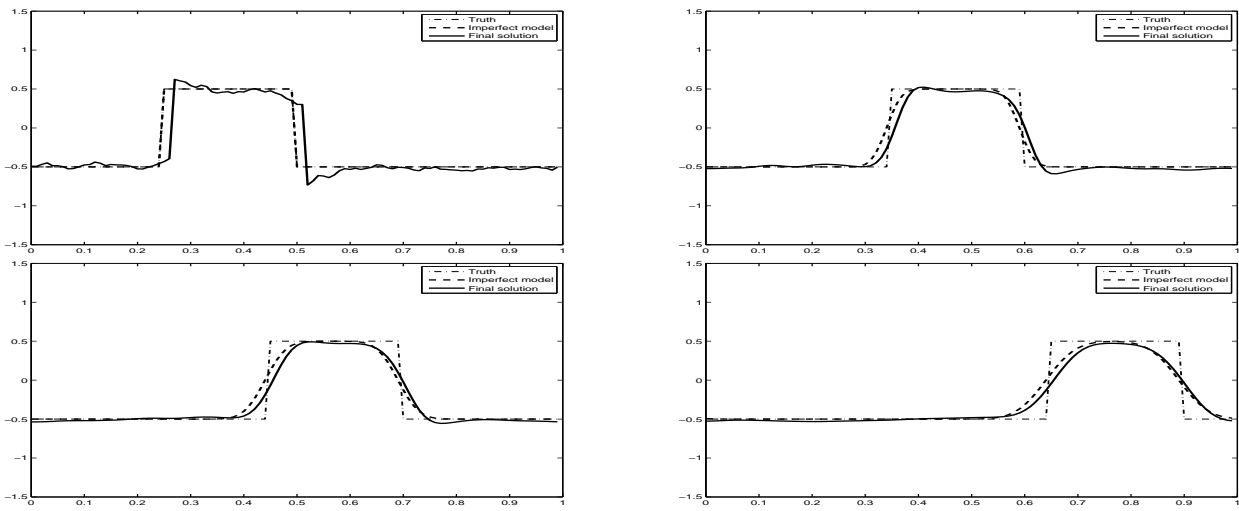


Figure 14. Results for 4DVar for a shifted (and noisy) background and for background error covariance matrix  $B$  taken from (29) with  $\sigma_b^2 = 0.01$

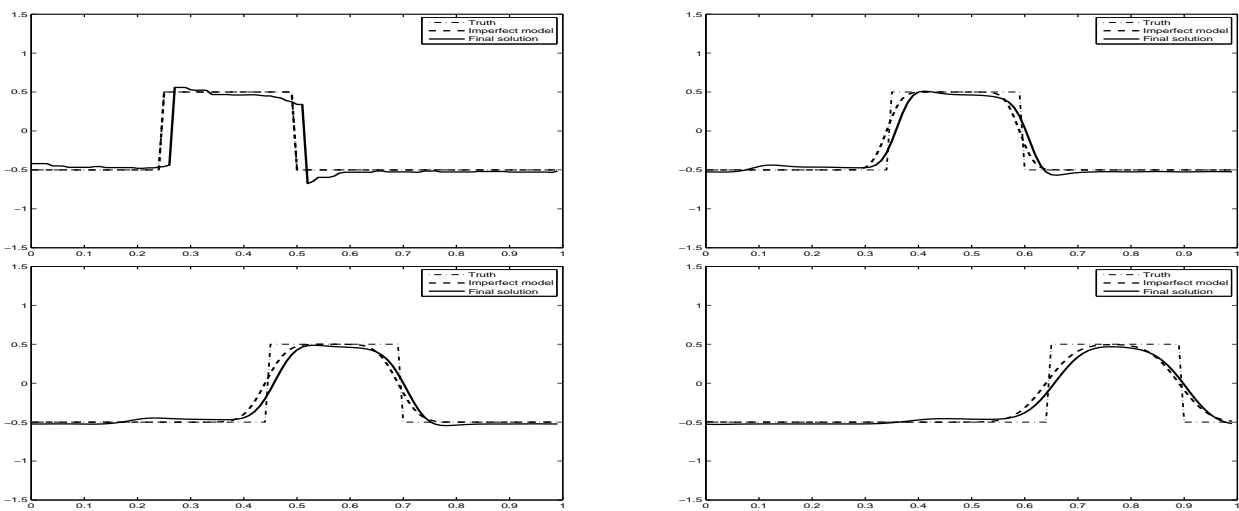


Figure 15. Results for mixed TV  $L_1$ - $L_2$ -norm regularisation for the same data as in Figure 14.

and 15. The initial condition in 4DVar is clearly recovered. Furthermore, at the end of the assimilation window the poorly, with many oscillations (see first plot in Figure 14). solution gives undershoots (see third plot in Figure 14)

and the amplitude of the front is reduced (see second and third plot in Figure 14). The solution at the initial time provided by the mixed TV  $L_1$ - $L_2$ -norm regularisation has less oscillation present in the shock wave (see first plot in Figure 15) and produces somewhat less distortion of the wave front over the window (see second and third plot in Figure 15). The errors in the analysis in this case for the standard 4DVar and the mixed TV  $L_1$ - $L_2$ -norm regularisation (with  $\delta = 10$ ) are similar, with a value of 1.80. Both methods smear the shock front and both produce an initial phase error which is reproduced in the forecast.

The plots in Figures 14 and 15 show that choosing an exponential (non-diagonal) covariance matrix  $B$  is not necessarily advantageous when there is a sharp front with a phase error. In this case both 4DVar and mixed TV  $L_1$ - $L_2$ -norm regularisation with a diagonal covariance matrix  $B$  capture the shock front more accurately, but the mixed TV  $L_1$ - $L_2$ -norm technique also eliminates the oscillations in the analysis arising from the effects of the model error (see Figures 12 and 13).

In general, the mixed norm approach removes oscillations and sharpens fronts - but the position of the shock is not recovered precisely where there is a phase error in the background.

## 6.2 A slanted front for the background

Finally, with the same experimental data as in Subsection 5.1 we consider a slanted background given by the slanted square wave

$$u_1^b(x, 0) = \begin{cases} -0.5 + \frac{50}{7}(x - 0.18), & 0.18 < x < 0.32 \\ 0.5, & 0.32 \leq x \leq 0.43 \\ 0.5 - \frac{50}{7}(x - 0.43), & 0.43 < x < 0.57 \\ -0.5, & x \leq 0.18, x \geq 0.57. \end{cases} \quad (30)$$

This slanted background is plotted in Figure 16. We add

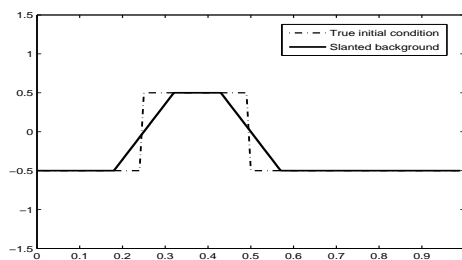


Figure 16. Slanted background (without noise) for Example in Section 6.2.

noise to this background, taken from a normal distribution with covariance matrix  $B$  taken from (29) with  $\sigma_b^2 = 0.1$ , which is consistent with the error between  $u_1^b$  and the true initial condition given by (28).

Figures 17 (4DVar) and 18 (mixed TV  $L_1$ - $L_2$ -norm regularisation) show the results where the background is given by (30). 4DVar produces oscillations in the initial condition (first plot in Figure 17) and is not able

to recover the correct initial condition from the (wrong) slanted background. The mixed TV  $L_1$ - $L_2$ -norm regularisation approach, however, does not generate oscillations in the initial condition (first plot in Figure 18) and moreover produces a well-recovered front, given that the background was given by a (wrong) slanted front (compare the results in the first plot of Figure 18 with the background in Figure 16). The error in the analysis, measured in the  $L_2$ -norm, for the standard 4DVar method is 1.10, whilst the error in the mixed TV  $L_1$ - $L_2$ -norm method with  $\delta = 100$  is only 0.86, a clear improvement. Hence, we conclude that the mixed TV  $L_1$ - $L_2$ -norm regularisation removes oscillations and sharpens fronts and steep gradients, whereas standard 4DVar, even where smoothing is provided via the background covariance matrix, introduces oscillations where the background frontal gradient is incorrect.

## 7 Conclusions and future work

In this paper we have presented mixed TV  $L_1$ - $L_2$ -norm regularisation, a new approach for variational data assimilation. We have given numerical examples containing shock fronts in order to demonstrate that mixed TV  $L_1$ - $L_2$ -norm regularisation gives better results than either the standard 4DVar ( $L_2$ -norm regularisation) technique or a simple  $L_1$ -norm regularisation technique in the presence of model error. The errors in the analysis at time  $t = 0$  are found to be consistently smaller for mixed TV  $L_1$ - $L_2$ -norm regularisation than for standard 4DVar or  $L_1$ -norm regularisation for a range of ratios of observation to background variance and for both perfect and noisy observations with various temporal and spatial frequencies. These examples demonstrate that, even where the noise in the background and observations is Gaussian with known covariances, the standard 4DVar approach does not produce as accurate an analysis as mixed TV  $L_1$ - $L_2$ -norm regularisation in the presence of sharp fronts and model error.

One of the strengths of the mixed TV  $L_1$ - $L_2$ -norm regularisation is that in the case where the background covariance matrix  $B$  is poorly tuned, it gives a much better performance than 4DVar in the presence of model error. This is relevant to operational NWP where the matrix  $B$  is difficult to determine and must, in any case, be simplified to make the assimilation problem computationally tractable.

Future work will be to apply this technique to higher dimensional and possibly multi-scale problems. Because the minimisation process for the mixed TV  $L_1$ - $L_2$ -norm regularisation approach in (19) is more involved than that for the standard approach in (13), practical implementations will also have to be investigated together with the efficiency of this new approach.

## Appendix

The solution to the the data assimilation problem can be interpreted in statistical terms, where certain assumptions

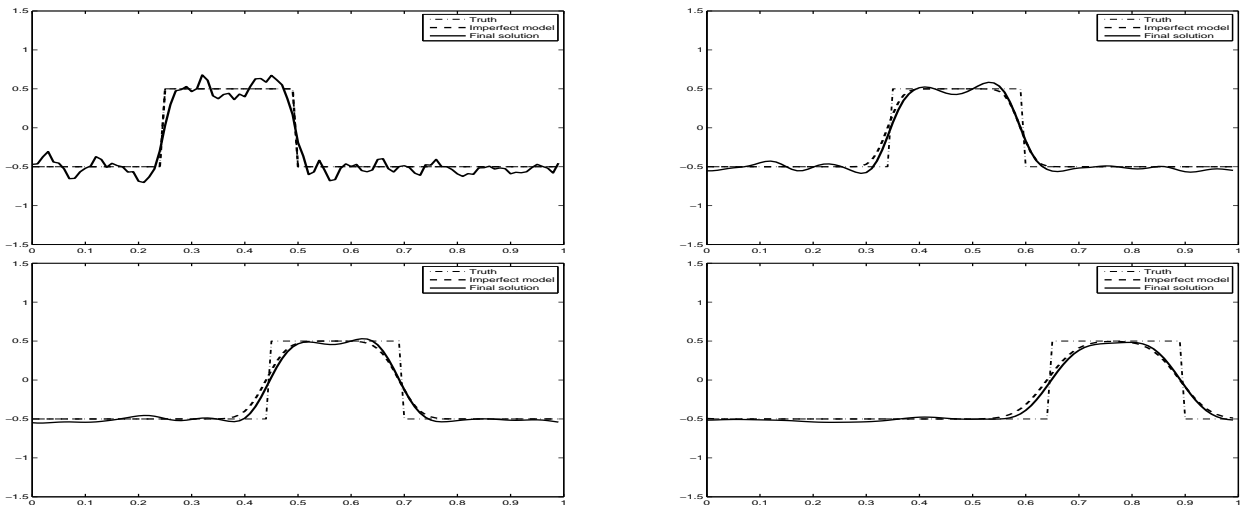


Figure 17. Results for **4DVar** for a slanted (and noisy) background taken from (30).

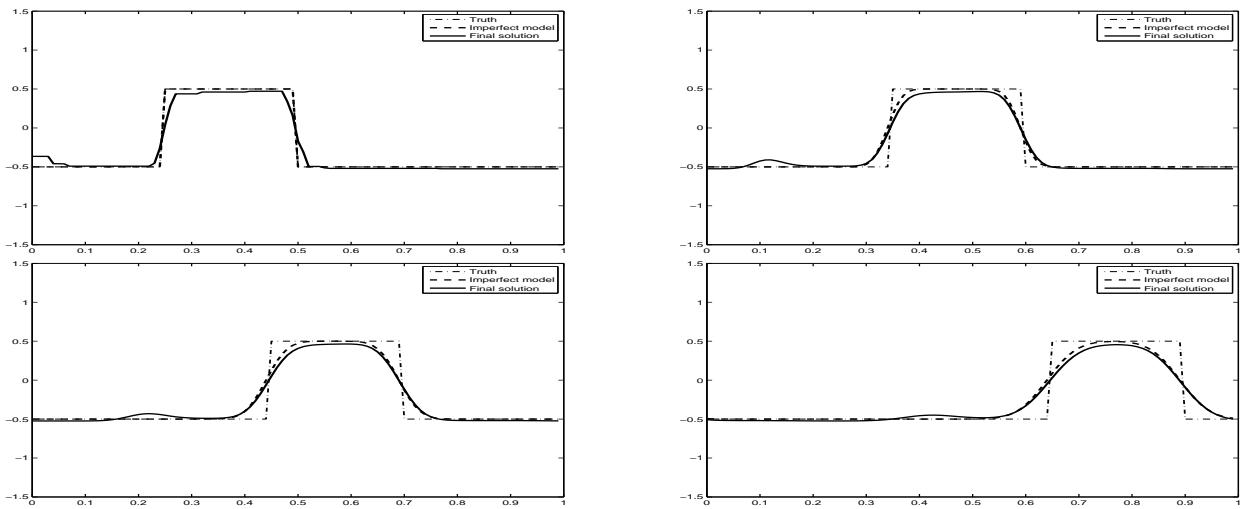


Figure 18. Results for **mixed TV  $L_1$ - $L_2$ -norm regularisation** for a slanted (and noisy) background taken from (30).

about the errors hold (Nichols (2010)). For the standard 4DVar problem, Gaussian errors are assumed for both the background and the observations, so the minimisation of the objective function (1) is equivalent to maximising the *a posteriori* likelihood estimate of the state, given the observations and the prior. A similar derivation can be made for  $L_1$ -norm regularisation (16) (which we are going to do here for the single variate case).

The addition of the penalty term  $\mu^2 \|z\|_1$  in (16) to the least squares term is sometimes also referred to as Lasso regression in statistics (Tibshirani (1996)). Now,  $|z_i|$ , where  $z_i$  is the  $i$ th entry of  $z$ , is proportional to the negative log-density of the Laplace (or double-sided exponential) distribution. Hence, the  $L_1$ -norm regularisation can be derived as a Bayesian posterior estimate, where the priors are independently distributed variables with Laplace probability density function

$$f(z_i) = \frac{1}{2\gamma} e^{-\frac{|z_i|}{\gamma}}, \quad (31)$$

where  $\gamma = 2/\mu^2$ . The in-depth mathematical investigation of  $L_1$ -norm regularisation is the subject of future research and beyond the scope of this paper.

In order to solve equation (3) at each step we use a direct matrix decomposition method (Gaussian elimination).

We remark that the solution of the minimisation problem using the least mixed norm solution described in section 4, (see also (Fu *et al.* (2006))) is more expensive than standard 4DVar as the problem size is increased. More efficient methods need to be found for the minimisation; the details are beyond the scope of this paper.

We note that traditional 4DVar is not designed to deal with model error. Hence, for future work, a fairer comparison would be weak-constraint 4DVar (see, for example Trémolet (2006)) with mixed TV  $L_1 - L_2$ -regularisation.



## Acknowledgement

The authors thank Nathan Smith (University of Bath) for helpful discussions on the subject of  $L_1$ -norm regularisation. The research of the first and third author is supported by Great Western Research (GWR) Grant "Numerical weather prediction: multi-scale methods and data assimilation" and by the Bath Institute for Complex Systems (BICS, EPSRC Critical Mass Grant). The research of the second author is supported by the National Centre for Earth Observation (NCEO).

## References

- Agarwal V, Gribok AV, Abidi MA. 2007. Image restoration using  $L_1$  norm penalty function. *Inverse Probl. Sci. Eng.* **15**(8): 785–809.
- Bennett A. F. 2002. *Inverse Modelling of the Ocean and Atmosphere* (234 pp.). Cambridge: Cambridge University Press.
- Daley R. 1991. *Atmospheric Data Analysis* (457 pp.). Cambridge: Cambridge University Press.
- Dennis Jr JE, Schnabel RB. 1983. *Numerical methods for unconstrained optimization and nonlinear equations*. Prentice Hall Series in Computational Mathematics, Prentice Hall Inc.: Englewood Cliffs, NJ, ISBN 0-13-627216-9.
- Donoho DL. 2006a. Compressed Sensing. *Information Theory, IEEE Transactions on* **52**(4): 1289–1306.
- Donoho DL. 2006b. For most large underdetermined systems of linear equations the minimal  $l_1$ -norm near solution approximates the sparsest solution. *Comm. Pure and Applied Maths* **59**(10): 907–934.
- Engl H, Hanke M, Neubauer A. 1996. *Regularization of inverse problems*. Kluwer Academic Pub.
- Fu H, Ng MK, Nikolova M, Barlow JL. 2006. Efficient minimization methods of mixed  $l_2$ - $l_1$  and  $l_1$ - $l_1$  norms for image restoration. *SIAM J. Sci. Comput.* **27**(6): 1881–1902 (electronic).
- Gill PE, Murray W, Wright MH. 1981. *Practical Optimization*. Academic Press, London, UK.
- Griffith AK, Nichols NK. 2000. Adjoint methods in data assimilation for estimating model error. *Flow Turbul. Combust.* **65**(3-4): 469–488.
- Haben SA, Lawless AS, Nichols NK. 2010. Conditioning and preconditioning of the variational data assimilation problem. *Computers & Fluids*, in press. (Published on line: 30 Nov 2010 doi:10.1016/j.compfluid.2010.11.025).
- Hansen PC. 1998. *Rank-deficient and discrete ill-posed problems*. SIAM Monographs on Mathematical Modeling and Computation, Society for Industrial and Applied Mathematics (SIAM): Philadelphia, PA, ISBN 0-89871-403-6. Numerical aspects of linear inversion.
- Hansen PC, Nagy JG, O'Leary DP. 2006. *Deblurring images, Fundamentals of Algorithms*, vol. 3. Society for Industrial and Applied Mathematics (SIAM): Philadelphia, PA, ISBN 978-0-898716-18-4; 0-89871-618-7. Matrices, spectra, and filtering.
- Johnson C. 2003. *Information Content of Observations in Variational Data Assimilation*. PhD Thesis. University of Reading.
- Johnson C, Nichols NK, Hoskins BJ. 2005. Very large inverse problems in atmosphere and ocean modelling. *Internat. J. Numer. Methods Fluids* **47**(8-9): 759–771.
- Lawless AS, Gratton S, Nichols NK. 2005a. An investigation of incremental 4D-Var using non-tangent linear models. *Q. J. R. Meteorol. Soc.* **131**: 459–476.
- Lawless AS, Gratton S, Nichols NK. 2005b. Approximate iterative methods for variational data assimilation. *Internat. J. Numer. Methods Fluids* **47**(10-11): 1129–1135.
- LeVeque R. 1992. *Numerical methods for conservation laws*. Birkhäuser.
- Lewis J, Lakshmivarahan S, Dhall S. 2006. *Dynamic data assimilation: a least squares approach*. Cambridge Univ Pr.
- Lorenc AC. 1981. A global three-dimensional multivariate statistical interpolation scheme. *Mon. Wea. Rev.* **109**: 701–721.
- Lorenc AC. 1986. Analysis methods for numerical weather prediction. *Q. J. R. Meteorol. Soc.* **112**: 1177–1194.
- Matlab R2012a Documentation, Optimization Toolbox. 2012. <http://www.mathworks.co.uk/help/toolbox/optim/ug/quadprog.html>.
- Morton K, Mayers D. 2005. *Numerical solution of partial differential equations: an introduction*. Cambridge Univ Pr.
- Nichols NK. 2010. Mathematical concepts of data assimilation. In: *Data Assimilation Making Sense of Observations*, Lahoz W, Khattatov B, Menard R (eds). Springer, pp. 13–39.
- Sasaki Y. 1970. Some basic formalisms in numerical variational analysis. *Mon. Wea. Rev.* **98**: 875–883.
- Schmidt M, Fung G, Rosales R. 2007. Fast optimization methods for  $l_1$  regularization: A comparative study and two new approaches. In: *ECML'07: Proceedings of the 18th European conference on Machine Learning*. Springer-Verlag: Berlin, Heidelberg, ISBN 978-3-540-74957-8, pp. 286–297.
- Strong D, Chan T. 2003. Edge-preserving and scale-dependent properties of total variation regularization. *Inverse Problems* **19**(6): 165–187.
- Talagrand O. 1981. A study of the dynamics of four-dimensional data assimilation (initial conditions specification for numerical weather prediction). *Tellus* **33**: 43–60.
- Tibshirani R. 1996. Regression shrinkage and selection via the lasso. *J. Roy. Statist. Soc. Ser. B* **58**(1): 267–288.
- Trémolet Y. 2006. Accounting for an imperfect model in 4D-Var. *Q. J. R. Meteorol. Soc.* **132**: 2483–2504.
- Wright SJ, Nowak RD, Figueiredo MAT. 2009. Sparse reconstruction by separable approximation. *IEEE Trans. Signal Process.* **57**(7): 2479–2493.